TECHNICAL RESEARCH REPORT

A Comparative Machinability Study of Dental Materials

by G. Zhang, D. Rekow, V. Thompson

T.R. 97-43

ISR

INSTITUTE FOR SYSTEMS RESEARCH

A COMPARATIVE MACHINABILITY STUDY
OF DENTAL MATERIALS

Guangming Zhang
Department of Mechanical Engineering
& Institute for Systems Research
University of Maryland
College Park, Maryland 20742

Dianne Rekow
Department of Orthodontics, Dental School
University of Medicine and Dentistry of New Jersey
Newark, New Jersey 07103

Van Thompson
Department of Restorative Dentistry, Dental School
Universit of Maryland at Baltimore
Baltimore, Maryland 21201

ABSTRACT

This paper presents results obtained from a comparative machinability study of newly invented ceramic materials for dental restorations. With the microstructure being the dominant factor on crack initiation and propagation during the fabrication process, the objective of this study is to identify the relationship between the microstructural characteristics and damage created during machining which could compromise the reliability of ceramic-made dental restorations. Glass ceramic material with tailored characteristics of microstructure is used in this study. The machining platform is milling operations where proper tool geometry and machining parameters are selected. Empirical models to correlate the cutting force and degradation of flexure strength with machining parameters are established. The aims of the research are to reduce surface cracking to yield improved surface finish (smoothness < 2 μm) and to lessen strength degradation after machining. The study consists of four steps, including characterization of microstructure, identification of machining parameters, on-line monitoring of the machining operations, and evaluation of flexure strength degradation. Contributions of this study are the establishment of a procedure for carrying out the machinability assessment, and the establishment of empirical models relating the cutting force and fracture strength degradation to the cutting conditions.

1. INTRODUCTION

As industry needs continue to push the performance limits of metals, more and more research is being conducted to take advantage of the superior properties of advanced ceramics, such as higher strength-to-mass ratio, and higher resistance to severe environments such as heat, wear, and corrosion. These outstanding qualifications of ceramics have led to their uses in wide-ranging applications where performance and reliability must be ensured. Yet, for all the potential that ceramics offer, the question remains in how to best process these materials during the fabrication of dental restorations. The material removal process in ceramics, unlike that of common metals and plastics, is characterized by micro-cracking and brittle fracture. Consequently, a machined ceramic part tends to possess micro-scale cracks and to fail at a reduced fracture strength during service.

In this research, a ceramic material called DICOR/MGC, commercially available, is chosen for the study. It is also called a machinable glass ceramic (MGC) which was developed at Corning Glass Works [Grossman, 1973]. The chemical makeup of DICOR/MGC consists of SiO_2, K_2O, MgO, Al_2O_3, and ZnO_2. During the heat treatment process, micaceous crystals are formed to give DICOR/MGC its strength and machinability. This crystalline phase is composed of tetrasilicic fluoromica, $K_2Mg_5Si_8O_{20}F_4$, and makes up about 50% of the ceramic [Giordano, 1996]. The size and shape of these crystals, or mica flakes, are controlled by the heat treatment process, of which the most critical factor is the temperature of heat treatment. Under different temperatures, the size of these elongated, cylindrical grains may vary from 1 μm to 10 μm in platelet sizes. The difference in microstructure in terms of the size provides variation of mechanical properties of the material. Table 1 lists the three types of DICOR/MGC manufactured from three different heat treatment temperatures and their corresponding fracture strength values [National Institute of Standards and Technology, 1996]. As illustrated in Table 1, the DICOR/MGC material under the heat treatment temperature of 1000 °C has the smallest grain size among the three with average mica platelets of 1.1 μm in size, called as possessing fine microstructure in this study. On the other hand, the

DICOR/MGC material under the heat treatment temperature of 1120 °C has the largest grain size with average mica platelets of 10.0 µm, called as possessing coarse microstructure in this study. Examining the difference in mechanical properties, the material with fine grain structure has the highest fracture strength ranging from 240 MPa to 280 MPa, and the so-called coarse material has the lowest fracture strength ranging from 115 MPa to 175 MPa [National Institute of Standards and Technology, 1996].

Table 1. Some mechanical properties of DICOR/MGC

Nomenclature	Heat Treatment Temperature (°C)	Mica Platelet Size (µm)	Fracture Strength (MPa)
Fine	1000	1.1	240-260
Medium	1060	3.7	210-245
Coarse	1120	10.0	115-175

2. BASIC METHODOLOGY

The basic methodology used in this research consists of four steps, as illustrated in Figure 1.
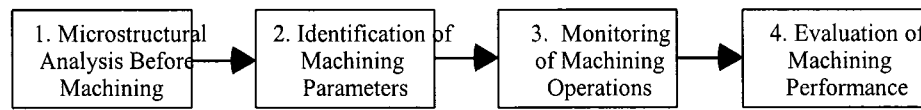

Figure 1. Basic methodology

1) Microstructural Evaluation before Machining: Each material, prepared in both raw (non-polished) and polished form, is examined using an Environmental Scanning Electron Microscope(ESEM) before machining. All of the prepared specimen are ultrasonically cleaned, and etched to optimize the conditions for machining tests. To minimize possible variations caused by the initial status of specimens, a unified polishing process is enforced to prepare all the specimens. Half of the polished specimens will be used for machining tests. And the other half of the specimens are not being machined and reserved for the purpose of comparison.

2) Machining Experiments: The method of using a 2^3 fractional factorial experiments is applied to study the main effects, as well as effects of interactions. The three selected machining parameters are spindle speed, feed, and depth of cut during machining. Force signals generated in the feed and transverse directions from the material removal process are recorded and analyzed using a PC computer system powered by LabVIEW software. An empirical model, characterizing the main effects, and interaction effects relating the cutting force to the machining condition, is developed for each of the three types of microstructural characteristics of the DICOR material. .

3) Fracture Strength Evaluation of the Specimens before and after Machining: Bi-flexural strength tests are performed on all the specimens before and after machining. Comparison between these results presents the strength degradation associated with individual machining conditions. Empirical models are developed to characterize the main effects, and interaction effects related to the strength and the machining conditions.

4) Data Analysis: Special efforts are made to study the interplay between the flexure strength degradation, the cutting force generation during machining and the applied machining conditions, thus leading to the identification of correlation between the microstructure, cutting force generation and the strength degradation.

2.1   Microstructural Analysis

Microstructure plays a significant role in governing the machining behavior of ceramics, in terms of its susceptibility to machining-induced surface and subsurface cracking. Therefore, a clear understanding of the microstructural aspect of each material, such as the grain size, orientation, and boundary relations are necessary to interpret machining results. Figure 2 illustrates a computerized image processing system used in this study [Zhang, 1994]. As illustrated, the process begins with a prepared specimen, either raw(non-polished), or polished. The specimens are 28 mm long bars with rectangular cross-section measured as 6 mm wide and 4 mm high x 28 mm. The specimen is placed into the environmental scanning electron microscope (ESEM) where microstructural images at magnification of 2500x can be clearly observed. The captured images of 640 pixels x 640 pixels are saved in a digital format, stored in the computer system, and can be retrieved for microstructural analyses.
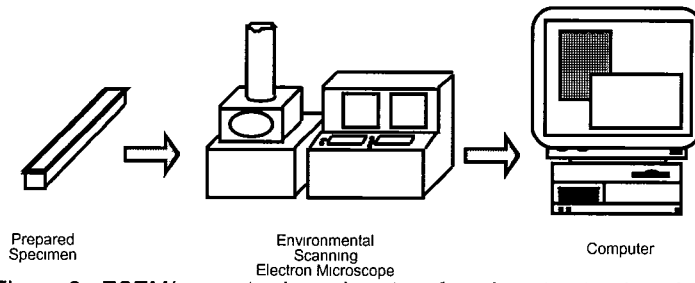
2

Figure 2. ESEM/computer-based system for microstructural analysis

Figure 3 presents SEM micrographs obtained from the performed microstructural analyses. The two columns represent the information before and after machining. The three rows represent the three types of microstructural characteristics, namely, DICOR/MGC-Fine, DICOR/MGC-Medium, and DICOR/MGC-coarse materials, respectively.
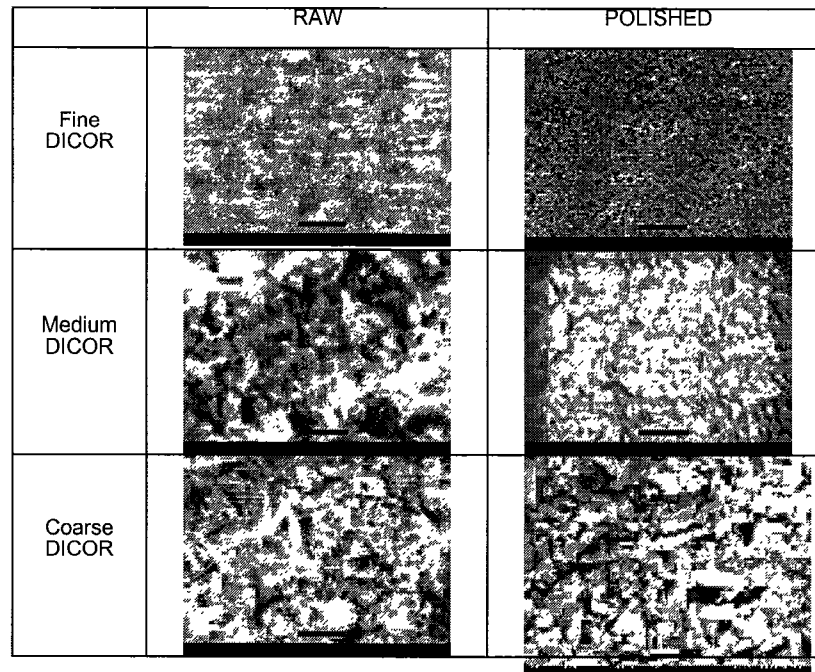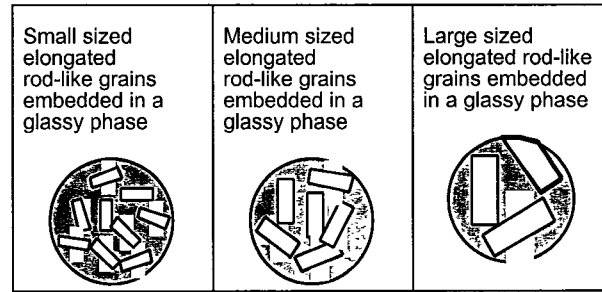

Figure 3. Microstructures of Dental Ceramics

As shown in Figure 3, the polished specimens produce better results than those of the non-polished specimen in terms of grain size, grain shape and grain boundaries. For example, the grains of the DICOR material are characterized by elongated rod-like structures of varying sizes, depending on whether the material is fine, medium, or coarse. As expected, the micrographs show that fine and coarse DICOR contain the smallest and largest grains, respectively, while the medium DICOR is somewhere in between. The visual evidence also reveals that these grains are suspended in a glassy phase, as shown most dramatically by the medium DICOR micrograph under the "polished" column in Figure 3. Thus, for DICOR, its microstructural features are characterized by grains of similar shapes but of different sizes, and by the existence of a two-phase structure. Table 2 is a summary of the microstructural characteristics observed for the DICOR/MGC-Fine, DICOR/MGC-Medium, and DICOR/MGC-coarse materials.

Table 2. Microstructural features of DICOR/MGC

DICOR/MGC		
Fine	Medium	Coarse

3

Small sized elongated rod-like grains embedded in a glassy phase	Medium sized elongated rod-like grains embedded in a glassy phase	Large sized elongated rod-like grains embedded in a glassy phase

2.2   Machining Experiments

Machining experiments, in the form of end milling, are conducted on the DICOR/MGC-Fine, DICOR/MGC-Medium, and DICOR/MGC-coarse materials.   A 2-level, 3-variable, factorial design of experimentation is illustrated in Figure 4 [DeVor, 1992]. The three machining variables are spindle speed, feed rate, and depth of cut. The upper and lower levels for each of the three machining variables are listed below:

		Spindle Speed (rpm)	Feedrate (mm/min)	Depth of Cut (mm)
Upper Level	(+)	900	30	0.19
Lower Level	(-)	600	20	0.12

Table 3 lists a design matrix and Figure 4 depicts the set of eight tests for each of the DICOR/MGC-Fine, DICOR/MGC-Medium, and DICOR/MGC-coarse materials. Therefore, a total of 24 machining tests are performed in this study.

Table 3. Design Matrix

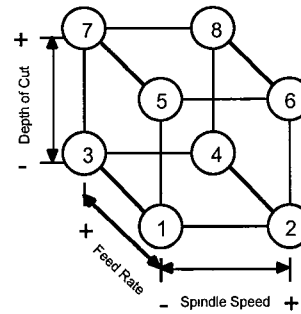| TEST	VARIABLE			
	Spindle Speed	Feed Rate	Depth of Cut	Surface Preparation
1	-	-	-	-
2	+	-	-	+
3	-	+	-	+
4	+	+	-	-
5	-	-	+	+
6	+	-	+	-
7	-	+	+	-
8	+	+	+	+

Figure 4. Geometrical representation of the design matrix

The experimental setup for the machining experiments is shown in Figure 5. The rectangular bars are secured to a metal fixture by first placing them in slots which have been machined at evenly spaced locations, and second applying epoxy around the specimens to form a strong bond to the fixture. The machining is performed using a 6.35 mm-diameter end mill with one pass over each specimen. Note that the cutting force is decomposed into its orthogonal feed and transverse components. For clarity, the feed force refers to the force generated in the direction of the path that the end mill travels in its machining operation, while the transverse force is the force generated in the direction that is 90 degrees from the feed direction. During machining, these two force components are measured simultaneously by a dynamometer. Tables 4a, 4b, and 4c list the data obtained from recording the two cutting force components during the 24 machining tests.

2.3   Fracture Strength Measurements

The specimens after being machined are released from the metal fixture. As illustrated in Figure 6, four-
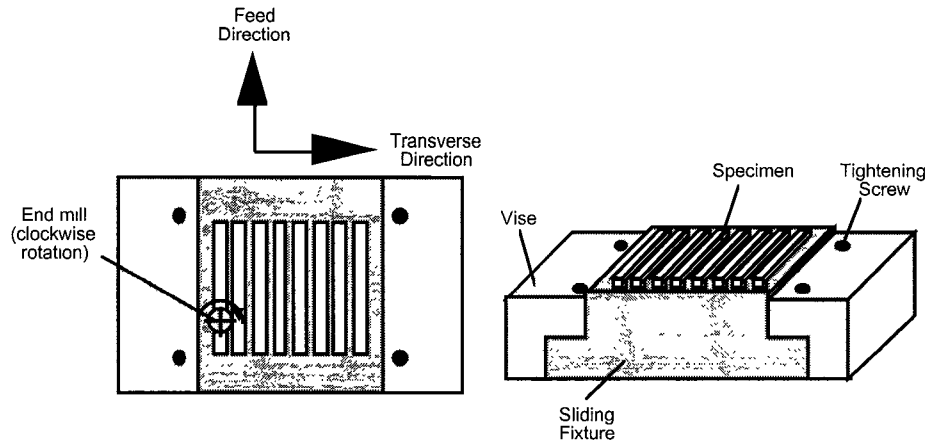
Figure 5. Vise-fixture system for machining

Table 4. Cutting Force Measurement Data

a) Fine DICOR					
	Machining Conditions				
Test #	Spindle Speed	Feed Rate	Depth of Cut	Feed Force [N]	Transverse Force [N]
1	-	-	-	15.59	3.05
2	+	-	-	2.19	0.86
3	-	+	-	3.34	2.26
4	+	+	-	11.98	3.46
5	-	-	+	1.38	2.56
6	+	-	+	6.95	4.95
7	-	+	+	7.44	7.37
8	+	+	+	3.12	3.19
b) Medium DICOR					
	Machining Conditions				
Test #	Spindle Speed	Feed Rate	Depth of Cut	Feed Force [N]	Transverse Force [N]
1	-	-	-	0.53	0.39
2	+	-	-	2.34	3.30
3	-	+	-	2.64	3.94
4	+	+	-	4.86	2.94
5	-	-	+	5.18	6.15
6	+	-	+	4.40	1.70
7	-	+	+	0.88	3.34
8	+	+	+	3.18	5.31
c) Coarse DICOR					
	Machining Conditions				
Test #	Spindle Speed	Feed Rate	Depth of Cut	Feed Force [N]	Transverse Force [N]
1	-	-	-	0.30	0.65
2	+	-	-	1.83	1.63
3	-	+	-	2.85	3.35
4	+	+	-	2.53	1.28
5	-	-	+	2.94	4.33
6	+	-	+	2.04	0.88
7	-	+	+	1.47	1.89
8	+	+	+	4.54	6.70

point bending tests are used to evaluate the fracture strength of those specimens after being machined, and those reserved specimens without being machined. The four-point bending tests are performed in parallel to block possible variations introduced to the measurement data. Table 5 presents the data obtained from these measurements. The three columns are used to distinguish the measurements from the DICOR/MGC-Fine, DICOR/MGC-Medium, and DICOR/MGC-coarse materials, respectively.
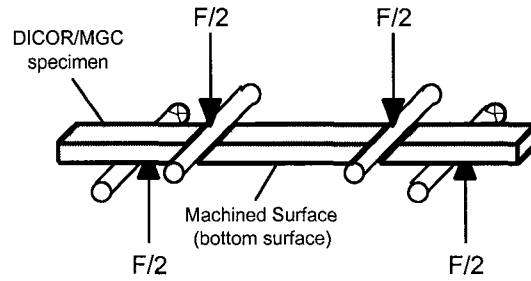
Figure 6. Four-Point Bending Tests to Evaluate Fracture Strength

Table 5. Fracture Strength Measurement Data

Fine DICOR/MGC				Medium DICOR/MGC			
Test #	Before Machining	After Machining	Difference	Test #	Before Machining	After Machining	Difference
1	260	47	213	1	225	41	184
2	260	49	211	2	225	89	136
3	260	34	226	3	225	66	159
4	260	47	213	4	225	34	191
5	260	44	216	5	225	75	150
6	260	45	215	6	225	66	159
7	260	41	219	7	225	62	163
8	260	31	229	8	225	62	163

Coarse DICOR/MGC			
Test #	Before Machining	After Machining	Difference
1	145	90	55
2	145	87	58
3	145	86	59
4	145	93	52
5	145	91	54
6	145	83	62
7	145	97	48
8	145	93	52

3. DATA ANALYSIS AND DISCUSSION OF RESULTS

3.1 Relation Between Cutting Force And Strength Degradation

Examining the cutting force data presented in Tables 4a, 4b, 4c, the three maximum cutting force components of feed force are 16 Newtons, 6 Newtons, and 5 Newtons for the DICOR/MGC-Fine, DICOR/MGC-Medium, and DICOR/MGC-coarse materials, respectively. These three maximum force components were measured when machining the DICOR/MGC-Fine at low spindle speed, low feedrate, and low depth of cut, machining DICOR/MGC-Medium at high spindle speed, high feedrate, and low depth of cut, and machining the DICOR/MGC-coarse at high spindle speed, high feedrate, and high depth of cut. Using the information and examining the data listed in Table 5, the corresponding fracture strengths of these specimens after machining can be identified as 47 MPa for the DICOR/MGC-Fine, 75 MPa for the DICOR/MGC-Medium, and 93 MPa for the DICOR/MGC-coarse, respectively. Figure 7a is the plot of these observation together with the fracture strengths measured from those specimens without being machined. Therefore, the plot clearly depicts the magnitudes of strength degradation for the three cases. The largest drop in fracture strength is 213 MPa associated with the DICOR/MGC-Fine, and the least drop is 47 MPa. Here the conclusion is the larger the cutting force component in the feed direction is generated, the severe degradation of the fracture strength can be anticipated.

The second observation is related to the data analysis of the cutting force components in the transversal direction. Figure 7b is the plot of the cutting force components in the transversal direction corresponding to the three maximum cutting force components of feed. They are 3 Newtons, 6 Newtons, and 6 Newtons for the
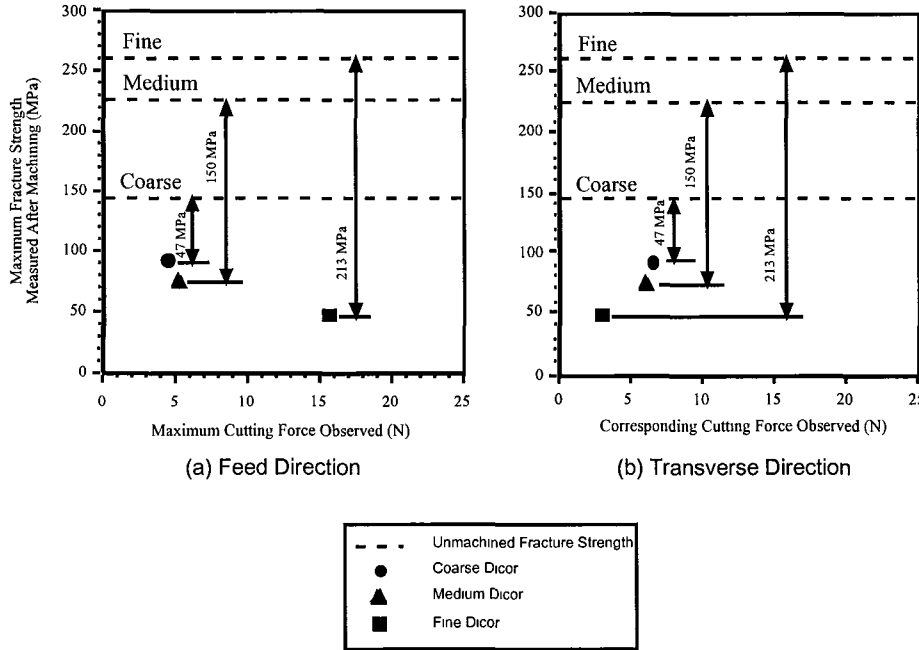
Figure 7. Fracture strength degradation of three types of DICOR/MGC for the a) feed and b) transverse directions

DICOR/MGC-Fine, DICOR/MGC-Medium, and DICOR/MGC-coarse materials, respectively. The variation among the three values is 3 Newtons, which is rather smaller than the variation among the three cutting force components in the feed direction, which is 11 Newtons. From comparing the two variations, it is evident that the dramatic drop of the fracture strength degradation of the DICOR/MGC-Fine material is mainly due to the presence of a significant large value of the cutting force component in the feed direction, which is 16 Newtons. This observation is important because it indicates the possible existence of a threshold stress value, above which cracking will be initiated and propagated in a much faster rate during machining. It is important to point out that using the magnitude of cutting force components in the transversal direction may not be as sensitive as using the component in the feed direction in evaluating the fracture strength degradation.

The third observation from this study is "how to assess the machinability among the DICOR/MGC-Fine, DICOR/MGC-Medium, and DICOR/MGC-coarse materials?" The data presented in this paper could lead readers to think that the DICOR/MGC-Coarse material possesses the best machinability because the fracture strength of the material in its final stage, or after being machined, remains at the highest level if comparing with those associated with the DICOR/MGC-Fine and DICOR/MGC-Median materials. However, the machining conditions explored in this study are very limited. Further investigations to look at the machining performance under machining conditions different from what has been used are imperative. In addition, interplay between the grain size and the machining condition applied is so complicated that DICOR/MGC materials with various grain sizes, especially between 5 μm to 10 μm in platelet sizes, are needed to further search those machining conditions, under which higher strength levels could be reached.

3.2 Empirical Models of Cutting Conditions to Cutting Force

With the observations of the cutting force and flexural strength established in the previous section, empirical models for the cutting force and flexural strength are presented next. The empirical models are based on the main and interaction effects as listed in Table 6. In the table, the subscript numbers 1, 2, and 3 refer to the spindle speed (S), feed rate (F), and depth of cut (D), respectively. To form the relationships, the mathematical model associated with a 2^3 factorial design is used. The model is defined as the linear combinations of the machining parameters as follows:

$$F = b_0 + b_1 x_1 + b_2 x_2 + b_3 x_3 + b_{12} x_1 x_2 + b_{13} x_1 x_3 + b_{23} x_2 x_3 + b_{123} x_1 x_2 x_3 \quad (1)$$

Table 6. Main and interaction effects of machining parameters on the cutting force

a) Feed Direction

MATERIAL	E_0	E_1	E_2	E_3	E_{12}	E_{13}	E_{23}	E_{123}

fine DICOR	6.50	-0.88	-0.06	-3.55	3.04	1.50	1.17	-7.98
medium DICOR	3.25	1.89	0.28	0.32	1.37	-1.13	-3.04	0.17
coarse DICOR	2.31	0.85	1.07	0.87	0.53	0.24	-0.56	1.46

b) Transverse Direction

MATERIAL	E_0	E_1	E_2	E_3	E_{12}	E_{13}	E_{23}	E_{123}
fine DICOR	3.46	-0.70	1.22	2.11	-0.80	-0.20	0.31	-2.49
medium DICOR	3.38	-0.14	1.00	1.48	0.63	-1.10	-0.60	2.58
coarse DICOR	2.59	0.07	1.43	1.72	1.30	0.61	0.26	2.83

In equation (1), F is the response of the model, and the x_1, x_2, and x_3 are the machining parameters of spindle speed, feed rate, and depth of cut, respectively. The coefficients in the equation, b_1, ..., b_{123}, are related to the effects listed in Tables 6 by $b = E/2$; and b_0 is the average of the responses, or E_0.

Applying the model to the results in Tables 6, the following equations are derived for DICOR/MGC-fine (results for medium and fine are analogous):

$$F_{feed} \quad = 6.50 - 0.44S - 0.03F - 1.78D + 1.52SF + 0.75SD + 0.59FD - 3.99SFD \qquad (2a)$$
$$F_{transverse} = 3.46 - 0.35S + 0.61F + 1.06D - 0.40SF - 0.10SD + 0.16FD - 1.25SFD \qquad (2b)$$

Here, F_{feed}, and $F_{transverse}$ are the feed and transverse force responses; and S, F, and D represent the high (+1) and low (-) levels of the spindle speed, feed rate, and depth of cut, respectively. In equations (2), note that some of the coefficients are relatively small compared to the first term, or the average response, in each equation. In such cases, the effects of the parameters associated with those coefficients may be negligible due to random variations during the machining experiments. A standard treatment of determining whether an effect is significant is the use of a normal probability plot.

The usefulness of these empirical equations is that they serve as starting points in the search for optimized machining conditions that may yield satisfactory machining performance in terms of cutting force and flexural strength. For example, since it was shown in the previous section that the feed component of the cutting force has a more prominent effect on the flexural strength degradation after machining, a good optimization scheme would be to focus on the feed force.

It should be noted here that the relationships developed here are extracted from empirical data, and, because of this, any interpretation of the equations is limited to the range of the input, namely the high and low levels. Therefore, the results are restricted to a very narrow region, and insight into machining performance must be tempered. Furthermore, the statistical significance of these results would be improved if the experiments could be repeated.

4. EFFECTS OF MICROSTRUCTURE ON CUTTING FORCES, FLEXURAL STRENGTH AND SURFACE INTEGRITY

It should be clear now that the machining performances of the three DICOR/MGC materials are drastically different. Naturally, the question arises as to the underlying cause. As pointed out previously, the microstructure of ceramics is very important to the mechanical and physical behavior. Therefore, it is no surprise that the DICOR/MGC, based on three different microstructures in terms of grain size, should perform as they do.

Table 7 lists the average forces and flexural strengths recorded for the three DICOR/MGC materials. The average force and strength data referred to here represent the average response of the whole cube of eight tests. For example, the average feed force of 6.5 N for DICOR/MGC-Fine in Table 7 is the average of all the feed forces measured in the machining of the eight DICOR/MGC-Fine specimens. Thus, the feed force of 6.5 N can be though of as a function of S, F, and D. In this case, S = 750 rpm, F = 25 mm/min, and D = 0.155 mm.

Regarding the forces in Table 7, note that as the grain size is increased from fine (1.1 μm) to medium (3.7 μm) to coarse (10 μm), the feed component decreases in a dramatic way. On the other hand, the increase in grain size has very little effect on the transverse component, again, showing that the transverse component of the force is insensitive to different microstructures. As for the flexural strength, it is increased as the grain size is increased.

Table 7. Average forces and flexural strengths of DICOR/MGC

DICOR/MGC	Average Force (N)		Average Flexural Strength (MPa)
	Feed	Transverse	
Fine	6.50	3.46	42.11
Medium	3.25	3.38	61.81
Coarse	2.31	2.59	90.10

Based on these results, it would seem that optimization of machining performance is critically dependent not only on the machining parameters, but also on the microstructure of a material. The results seem to support the conclusion that large-grained DICOR/MGC facilitates the mechanism of material removal better than small-grained DICOR/MGC in terms of reducing cutting force generated during machining and of diminishing the flexural strength degradation after machining. Furthermore, it would seem that the small-grained DICOR/MGC is more fracture resistant due to its microstructure, but that the consequences are increased cutting forces, more surface damage, and reduced flexural strength after machining.

As a further example of the effects of microstructure on the machining performance, an examination of the machined surfaces of DICOR is necessary. In Figure 8, the fine, medium, and coarse materials are shown. These micrographs are typical of the types of surface features generated after machining. In Figure 8 (a), the fine material shows characteristics of micro-fracture. First, note that on the lower right side of the micrograph, the surface is relatively smooth and even (1). Contrasting this is the large volumes being removed (2), caused by the chip-forming process, an example of which is shown in (3). Finally, note the cracking that occurs ahead of the chip-forming process, as evidenced by (4). Assessment of these fracture-related features suggests that the material removal mechanism by which the fine material operates is one of crack propagation that results in large chip formation when several cracks meet to form the chip volume. However, the force required to propagate the cracks is high, which in turn generates high mechanical stress on the surface. Consequently, the result is uncontrollable fracturing and severe surface damage. This type of damage is consistent with DICOR/MGC-Fine.

Figure 8 (b) is a micrograph of a surface of a machined DICOR/MGC-Medium. Compared to the previous micrograph, one major difference is noticeable: the surface shows tracks left by the cutting tool (1), an indication that the material removal mechanism is somewhat less brittle. However, cracking that leads to brittle fracture is still the primary mechanism, as evident by the large volumes removed (2), brought about by chip formation (3) due to the propagation of cracks (4).

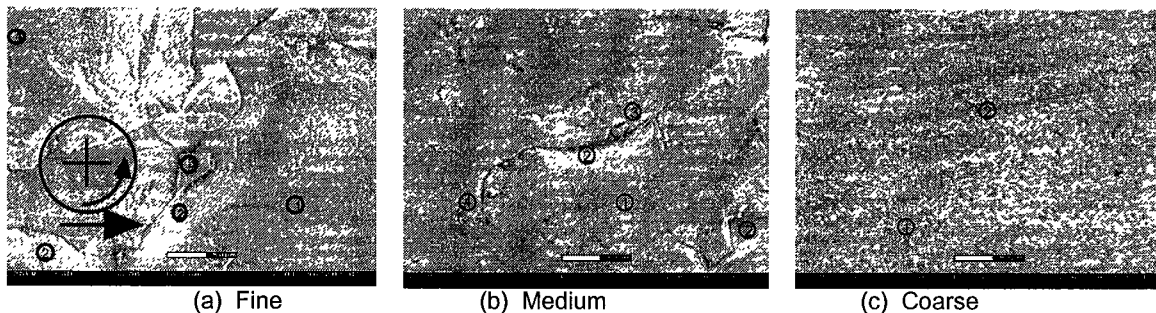(a) Fine   (b) Medium   (c) Coarse

Figure 8. ESEM micrographs (x 250) of machined DICOR/MGC surfaces

Lastly, Figure 8 (c) shows the machined surface of DICOR/MGC-Coarse. The micrograph is clearly different from the previous two in that there is no noticeable cracking (1). In fact, of the three materials, this material is most ductile-like because its machined surface shows very prominently the tracks left from the cutting tool path during machining (2). This is because the material removal mechanism of the coarse material is unlike that of the fine and medium materials. Figure 9 is a micrograph of higher magnification of the machined coarse material showing individual grains, which have been sheared in half. This is in fact the most likely mechanism of material removal mechanism in the coarse material. The grain-shearing phenomenon can best be described as transgranular cracking that leads to brittle fracture of the individual grains. From this perspective, then, it is easy to understand how the coarse material is more machinable of the three. It seems that the underlying principle governing the material removal mechanism of DICOR/MGC-Coarse is still cracking and brittle fracture; however, the mechanical stress that induces the failure is less because the cracking propagates through the grains and not through a tortuous path as may be the case with DICOR/MGC-Fine and DICOR/MGC-Medium. Since a significant
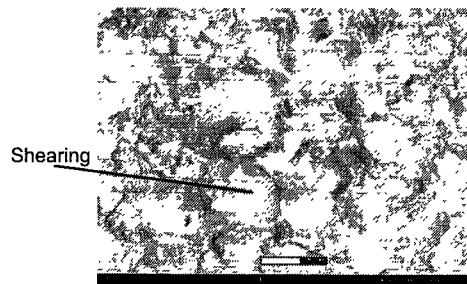

Shearing

Figure 9. Micrograph of DICOR/MGC-Coarse showing material removal mechanism

amount of the cracking is transgranular, subsurface damage is minimized and the flexural strength after machining is
not so drastically reduced.

In summary, results obtained from this study clearly indicate that microstructural characteristics of dental ceramics have dominant effects on their mechanical properties, thus leading to a variation of the response of the material to the machining process. To optimize the clinical performance of dental ceramics, a balance has to be made between the effort in material synthesis and the effort in identifying appropriate machining conditions to achieve the minimized strength degradation with a sufficiently high strength sustained after machining.

5.   CONCLUSIONS

This paper presents a research effort to perform a combined analytical and experimental study. The study is focused on identifying fracture strength degradation caused by micro-crack fracture induced during the machining of dental ceramics. Results obtained from this study clearly indicate that microstructural characteristics of dental ceramics have dominant effects on the material response to the machining process, thus leading to variation of the degradation of flexure strength. To optimize the clinical performance of dental ceramics, a balance has to be made between the effort in material synthesis and the effort in identifying appropriate machining conditions to achieve the minimized strength degradation with a sufficiently high strength sustained after machining.

References
Devor R., Chang T., and Sutherland J., Statistical Quality Design and Control, Macmillan Publishing, 1992.

Giordano, R. A., Dental Ceramic Restorative Systems, Compendum, Vol. 17, No. 8, 1996.

Groenou, A. B. V. and Veldkamp, J. D. B., "Grinding brittle materials," Machining Hard Materials, Society of Manufacturing Engineers, 1982.

Grossman, D. G.: Tetrasilicic mica glass-ceramic material, Washington, D.C.: US Patent Office, US Patent No. 3,732,087, 1973

Lawn B. R., Fracture of Brittle Solids, Cambridge University Press, Cambridge, 1993.

Le, D., Qi, L., Zhang, G., "Microstructural Effects on the Machining Performance of Dental Ceramics," Proceedings of 1997 ASME International Mechanical Engineering Congress and Exposition.

National Institute of Standards and Technology, Machinable Ceramics Monthly Report, 1996.

Ng, S., Le, D., Tucker, S., Zhang, G., "Characterization of Machine Induced Edge Chipping in Glass Ceramics," Proceedings of 1996 ASME International Mechanical Engineering Congress and Exposition.

Zhang, G. M., Ko, W. F. , and Ng, S. J., " Submerged Precision Machining of Ceramic Material", Proceedings of 1995 Joint ASME Applied Mechanics & Materials Conference, AMD-Vol. 208, pp. 65-79., 1994.

Zhang, G. M., Ng, S. J., & Le, D. T., " Characterization of Surface Cracking Formed during the Machining of Ceramic Material", Proceedings of 1995 ASME International Mechanical Engineering Congress and Exposition, MED-Vol., 2-1, pp. 415-429, 1995.